Geoinformation for European-wide Integration, Benes (ed.)

3D mapping with high-resolution images

Thierry Toutin
Natural Resources Canada, Canada Centre for Remote Sensing, Ottawa, Canada

René Chénier & Yves Carbonneau
Consultants TGIS inc., Montreal, Canada

Nicolas Alcaïde
Université Louis Pasteur, Illkirch, France

Keywords: high resolution, 3D parametric model, ortho-rectification, stereo DTM, 3D building extraction

ABSTRACT: High-resolution images, EROS-A1, IKONOS and QuickBird-2 from 2 m to 0.6 m pixel spacing respectively, are geometrically processed with a 3D parametric model developed at the Canada Centre for Remote Sensing. A positioning accuracy of one pixel for the ortho-images can be obtained if 7-10 ground control points (GCPs) used in the 3D parametric model computation are better than 1-pixel accurate (cartographic and image coordinates) and if the digital terrain model (DTM) used in the ortho-rectification process is more accurate than 5-m. When the GCPs are less accurate (around 3-5 m) 20 are necessary to avoid the error propagation through the 3D parametric model. Furthermore, a DTM is extracted from stereo IKONOS images using automatic image matching. A general accuracy of 6.5 m (68% level of confidence) when compared to an airborne lidar DTM (0.5 m accurate) is obtained but is correlated with the land covers. However, the accuracy on bare soils improves to 1.5 m (68% level of confidence). Since the surface heights are included in DTM, the surface and the height of buildings can be extracted from the stereo IKONOS DTM. Different methods are proposed, which should used an expert system to integrate *a priori* information on the buildings in the different processing steps.

1 INTRODUCTION

EROS-A1, IKONOS and Quickbird-2 are the three civilian satellites, which presently provide images with the highest resolution: the sensors can generate 1-m, 2-m and 0.6 m panchromatic images, respectively. They also have off-nadir viewing up-to-60º in any azimuth depending of the sensor, which improves the revisit rate of the same ground area to two and three days. These two principal characteristics (high resolution pixel and stereo) enable the use of traditional 3D photogrammetric techniques with the stereo-images to extract accurate planimetric and elevation information. Since IKONOS launch in December 1999, preliminary research studies demonstrate positioning accuracy of 1-3 m depending of the input data using 3D parametric model (Toutin and Cheng, 2000) or 3D non-parametric models (Fraser et al., 2001). In general, the restitution accuracy, which includes the extraction error, is in the order of 2-3 m. Sub-pixel accuracy is only obtained on limited number of check-points as very well-defined targets. Preliminary work on digital terrain models (DTM) shows also a good potential with accuracy of 3-5 m (Toutin *et al.*, 2001).

Other research studies addressed the extraction of buildings: (a) from high-resolution DTMs stereo-extracted from air photos (Weidner & Förstner, 1995), (b) from IKONOS using additional elevation information (Hofman, 2001) and (c) directly from stereo IKONOS images (Fraser et al., 2001).

This paper expands on the above-mentioned preliminary results with larger data set of panchromatic high-resolution images: EROS (2m), IKONOS (1 m) and QuickBird (0.61 m). Different topographic data and accuracy are used to geometrically process the images with a multi-sensor geometric model developed at the Canada Centre for Remote Sensing (CCRS), Natural Resources Canada (Toutin, 1995) and adapted to high-resolution images (Toutin and Cheng, 2000). This paper presents results using different high-resolution images on ortho-rectification, DTM generation from stereo images and the extraction of buildings from the stereo extracted DTM.

2 STUDY SITES AND DATA SETS

Six high-resolution images, including EROS and IKONOS stereo-pairs (base-to-height ratio of one), were acquired over four different study sites with low-to-hilly topography. The cartographic data are

the ground control points (GCPs) collected from differential GPS (DGPS) with an accuracy of 0.5 m in the three axes, except for the Ottawa and Beauport study sites. Ortho-photos with 5-m accuracy and 1-m accurate GCPs stereo-compiled from 1:40,000 scale photos are respectively used for these study sites. DGPS are in the process of acquisition. Most of DTM have 5 m grid spacing and 5-10 m accuracy (68% level of confidence), except for the Beauport study site with an airborne lidar DTM (0.5-m accuracy). Table 1 summarizes the study sites with their respective images and cartographic data. Figure 1 is an example of QuickBird image (350 x 350 pixels) Texas, resampled with 10-cm pixel spacing.

Table 1. Study sites and data sets

Study sites	Environment Type	Relief Delta Z	Images	Carto. Data (accuracy)
Tokyo	Urban	Flat	EROS	DGPS (.5m)
Japan		60 m		DTM (5m)
Toronto	Sub-urban	Flat	EROS	DGPS (.5m)
Canada		60 m	IKONOS	DTM (5m)
Beauport	Residential	Hilly	Stereo-	DGPS (1m)
Canada	Semi-rural	500 m	IKONOS	Lidar (.5m)
Ottawa	Urban	Hilly	Quick-	Photos (5m)
Canada	Rural	300 m	Bird	DTM (5m)
Texas	Urban	Flat	Quick-	DGPS (.5m)
USA		100 m	Bird	DTM (10m)

Figure 1. Sub-image (35 x 35 m) of QuickBird-2 over Texas, USA resampled with 0.10 m pixel spacing. QuickBird Image © DigitalGlobe 2002

3 IMAGE ORTHO-RECTIFICATION

Since the geometric processing of high-resolution images is roughly the same than for other images, the four key processing steps are only summarized:

1. Acquisition and pre-processing of the remote sensing data (image(s) and metadata) to determine an approximation of the 3D parametric model(s);
2. Acquisition of cartographic data: collection of GCPs with their 3D cartographic coordinates and 2D image coordinates (1-2 pixels accuracy);
3. Computation of the 3D parametric model(s), initialized with the approximate parameter values and refined by an iterative least-squares (stereo) bundle adjustment with the GCPs; and
4. Ortho-image generation with a DTM into the user cartographic projection.

The 3D parametric model is the model developed for multi-sensor images at CCRS (Toutin, 1995) and adapted for high-resolution images (Toutin and Cheng, 2000; Toutin, 2001). The model corresponds to the colinearity equations for VIR images. It further reflects the physical reality of the complete viewing geometry and corrects all geometric distortions due to the platform, sensor, Earth, that occur during imaging process, and also the deformations of the cartographic projection.

The first results are related to Step 3 with the verification of the 3D parametric model accuracy using independent check points (ICPs). Previous experiments demonstrated that 10 and 20 GCPs are enough to compute CCRS 3D parametric model of high-resolution images when the GCPs are better than 1 m and 3-5 m accurate, respectively (Toutin, 2001). The redundancy of GCPs in the least-squares adjustment enables the input errors to not be propagated in the 3D parametric model. Table 2 gives the root mean square (RMS) and minimum/maximum errors on ICPs for all image adjustments computed with limited amount of GCPs.

Table 2. Number of GCPs/ICPs, root mean square (RMS) and minimum/maximum errors (in metres) on the ICPs from the least-squares adjustment computed with GCPs.

Study sites Image (pixel)	GCP/ICP Number	RMS Errors X	RMS Errors Y	Min/Max Errors X	Min/Max Errors Y
Tokyo					
EROS (2m)	10/15	4.3	4.6	-7/7	-6/8
Toronto					
IKONOS (1m)	7/23	1.3	1.3	-3/3	-3/3
Beauport					
IKONOS (1m)	10/46	2.6	1.9	-10/10	-10/10
IKONOS (1m)	10/46	2.5	2.2	-10/10	-10/10
Texas					
QuickBird (.6m)	6/16	1.1	1.0	-2/2	-2/2
Ottawa					
QuickBird (.6 m)	20/37	5.1	6.0	-12/11	-16/14

When the cartographic coordinates were 0.5-m precise, RMS errors were around 1 m for QuickBird, 1-2 m for IKONOS and 4 m for EROS, which approximately correspond to two pixels for each image. The RMS errors reflect thus the different GCP plotting error on each image, while the cartographic error (0.5 m) is negligible in the overall error budget. When the cartographic coordinates were 5-m precise

(for Ottawa), the RMS errors were a little worse around 5 m. Consequently, the RMS errors reflect thus the cartographic coordinate errors (5 m) of this study site, while the plotting error on image (1-2 pixels) is almost negligible in the overall error budget. Consequently, the results of the bundle adjustment reflect the cartographic or plotting errors, which do not propagate through the 3D parametric model, but rather through the point residuals/errors.

4 DTM GENERATION

In the processing steps for DTM generation with high-resolution stereo images there are few more steps: the image matching to find conjugate points in the stereo images, the computation of the 3D cartographic coordinates and the editing. The image matching used a mean normalized cross-correlation method with a multi-scale strategy. The computation of the 3D coordinates used the previously computed stereo-model (coplanarity equations) of Step 3 and finally the editing used 3D semi-automatic and visual tools for processing the blunders, the mismatched areas and the hydrographic features to generate a topographically coherent DTM. These three steps are roughly the same than for other sensors.

The first results are given with the verification of the stereo-model accuracy for the two study sites (Tokyo and Beauport). Due to the limited number of stereo-points in EROS stereo-pair, only one test was realized with all 10 stereo-GCPs. However, three tests were realized to compute the stereo model for Beauport study site: all 55 GCPs, 10 GCPs/45 ICPs and 10 GCPs/45 ICPs including one erroneous point (20 m error in X-direction). Table 3 summarizes these results.

The tests with their consistent results show that GCP plotting errors (1-2 pixels) did not propagate in the parametric model but is reflected in the RMS residuals and errors.

Table 3. Number of GCPs/ICPs, root mean square (RMS) residuals/errors (in metres) on the GCPs/ICPs, respectively from the stereo-model adjustment computed with GCPs. *In italic*, the values are the errors for the erroneous point.

Study site/ Stereo-pair GCP/ICP Number	RMS Residuals X	Y	Z	(RMS) Errors X	Y	Z
Tokyo EROS 10/0	3.1	3.2	0.8			
Beauport IKONOS 55/0	1.9	1.7	2.2			
10/45	1.5	1.4	1.3	2.6	2.2	2.9
10/45 1 error GCP	5.1	1.5	1.5	*12*	*1.9*	*-1.3*

This remark is more obvious with the last test using an erroneous GCP: the X-error (*12 m*) of the erroneous GCP is two and half times higher than the RMS X-residual (5.1 m). Consequently, the systematic error is immediately detected with its approximate value and direction. Test 10/45 with IKONOS, whose error result are in the same order than Table 2, confirms that 10 GCPs are enough to achieve a restitution accuracy of 2-3 m, both in horizontal (circular error) and vertical (linear error) directions; this restitution accuracy includes the feature extraction errors and are thus an indication of the potential accuracy (positioning and elevation) of the future stereo-extracted DTM.

The second results are with the evaluation of the stereo extracted DTMs. For the Tokyo study site, it was almost impossible to match conjugate points due to long shadows and hidden parts (30° collection angle) generated by downtown skyscrapers. For the Beauport study site about 5,500,000 elevation points were compared to 1-m accurate airborne lidar DTM, and the elevation differences are used to compute elevation errors with 68% and 90% levels of confidence, LE68 and LE90, respectively and the bias. Preliminary evaluation (Toutin *et al.*, 2001) demonstrated that the elevation accuracy is a function of land covers and the surface height (or at least a part of) is included in the extracted elevation for buildings, forest canopy, large walls. In fact, DTM is a digital surface model (DSM). Figure 2 shows the DSM, where street patterns (A), roads (B) and power lines (C) can be perceived due to residential house or forest canopy heights, respectively.

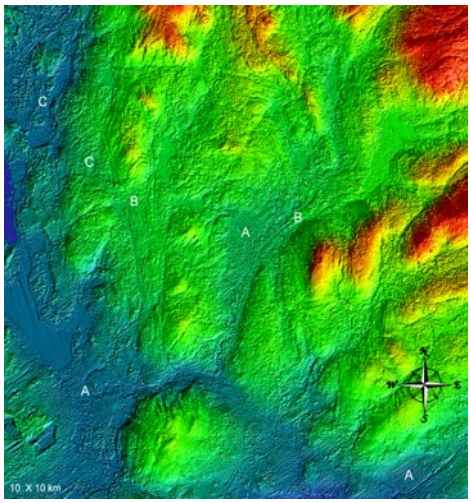

Figure 2. DTM extracted from stereo IKNOS images over Beauport, Canada. A, B and C are residential areas with street patterns, road corridors and power lines in forest, respectively.

In order to not be biased by the surface heights, the accuracy evaluation is specifically performed on bare soils. More results as a function of different land covers will be shown at EARSeL Symposium.

Table 4 summarizes the statistical results on the full DTM area and bare soils.

Table 4. Statistical results (in metres) with LE68 and LE90. bias, minimum and maximum errors computed from the difference between the stereo-extracted DTM and the lidar DTM.

ERRORS	LE68	LE90	Bias	Min./Max.
Full DTM area 5,500,000 points	6.5	10.0	6.0	-36/64
Bare soils 300,000 points	1.5	3.5	1.5	-23/32

Since about 65% of the area is covered by forest (deciduous, conifer, mixed and sparse), the results on the full DTM are mainly influenced by the height of tree canopy. Depending of the type of forests, the reflectance values of IKONOS images are representative of the top of canopy, between the top and the ground or even the ground, generating different bias or elevation errors. Consequently, unbiased estimation of the stereo-extracted DTM accuracy is better given by the results over bare soils: LE90 of 3.5 m corresponds to level-3/4 DTED and enables then 5 to 7 m contour lines to be generated according to level-1 NATO standard.

The last test was to compute the correlation between elevation accuracy of the DTM and the terrain slopes. Figure 3 show the LE68 and LE90 as a function of the slopes: the correlation coefficients R^2 of the linear regression are 0.86 and 0.96, respectively. The two curves and linear regression lines are almost parallel with about the same increasing rates (0.15 and 0.14, respectively).

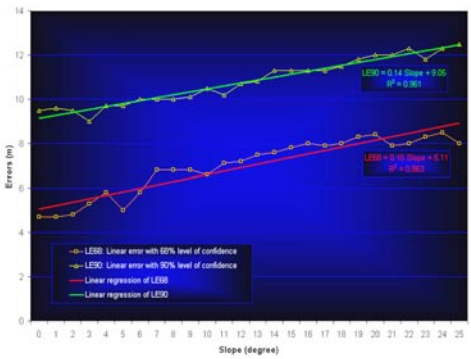

Figure 3. Results of DTM accuracy, LE68 and LE90 (in metres), when compared to 0.5-m lidar DTM as a function of the terrain slopes (degrees).

5 3D BUILDING EXTRACTION FROM DSM

As mentioned previously, DSM includes the height of surfaces, such as buildings. Figure 4 shows an area (100 m by 100 m; 1-m pixel spacing) for the IKONOS image (left) and the DSM (right). The shapes of industrial buildings are well recognizable and have similar shapes. Furthermore, the mean elevation of the building (158 m) gives approximate heights of 4 m and 11 m, when compared to the ground on the West and East sides, respectively. Both elevations and building heights are consistent with the reality (existing DTM and types of building). The line in Figure 4 is an elevation profile used to evaluate the next processing steps. Using information on the buildings (elevation, size, etc.) and their environment, two methods for the building extraction (shape and elevation) are presently under investigation.

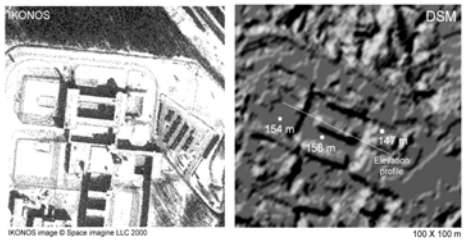

Figure 4. Sub-images of stereo-extracted DTM (left) and IKONOS (right) showing an industrial building. Profile line is used to verify the processing step results of building extraction. IKONOS Image © Space Imaging LLC, 2001

The first method intends "to sharp building edges" (edge regularization) in order to have elevation variations between the terrain and the buildings over the minimum of pixels and then uses the Fourier transformation to determine the boundaries of the buildings by only keeping the high-frequency elevation variations. Some filtering will also be applied in the Fourier domain. When converting back the results in the image domain, building elevations can easily be computed. The result of the first step is illustrated with elevation profiles before (blue red line) and after (red plain line) the regularization step (Figure 5). The West edges (elevation variation over ten pixels) of the building facing the sun illumination are not as sharp as the East edges (variations over 1-2 pixels). One reason could be that the building shadows, which generate sharp grey level differences in the images, enable a better image matching to be performed in these areas. However, the Fourier transformation will be a good tool for also extracting edge azimuths.

The second method processes the DSM into a smooth DTM to withdraw the surface elevation with large-window filtering. The difference between the DSM and this smooth DTM represents the surface heights after removing all negative values. Figure 6 shows the two profiles, before (blue red line) and after (red plain line), where the positive elevation differences approximately correspond to apparent building surfaces. In fact, true building surfaces

should correspond to the surface with the higher elevations because the building edges are not sharp, as mentioned in the first method. Consequently, information on the buildings (minimum and maximum heights, surfaces) is used to evaluate the difference between the apparent building surfaces and the true building surfaces. This information is also to delete some other surfaces (groups of trees, hedges, walls, etc.) and erroneous surfaces. A segmentation process is then applied on the last results to determine building edges and to compute their heights.

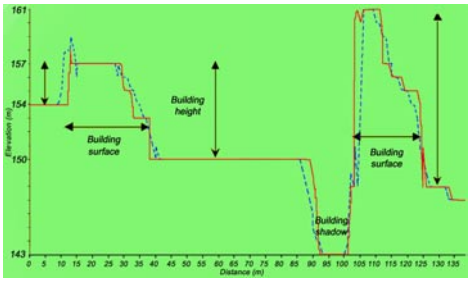

Figure 5. Elevation profiles before (blue dashed line) and after (red plain line) the building regularization to sharp building edges.

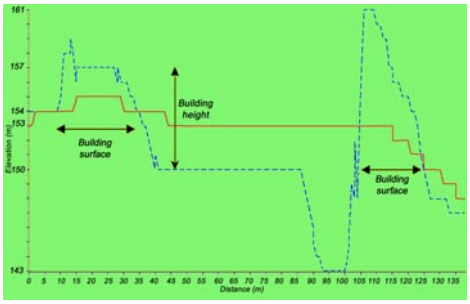

Figure 6. Elevation profiles before (blue dashed line) and after (red plain line) the DTM smoothing to withdraw the surface elevations.

Since *a priori* knowledge is useful to extract buildings an expert system should be used to determine the different buildings areas with their characteristics in a data base. More results on these two methods (mainly their second processing steps) and their combination will be presented at EARSeL Symposium with their potential applications in operational environment.

6 CONCLUSIONS

Different high-resolution satellite images (EROS-A1, IKONOS, QuickBird-2) have geometrically processed using DTM and CCRS 3D parametric modelling, which represents the colinearity and coplanarity conditions. As few as 6-10 GCPs can be used when they have an accuracy of 1-m or better and a final positioning accuracy of 1-2 pixels can be obtained. The major error in the error budget is the GCP plotting error on the image. On the other hand, twenty 2-3 m accurate GCPs are recommended to achieve 2-3 pixel positioning accuracy. The major error in the error budget is thus the GCP cartographic error.

In a second step, DTM has been extracted from stereo IKONOS images using an image-matching hierarchical algorithm. LE68 and LE90 of 6.5 m and 10 m respectively, were achieved for the full DTM. Since the elevation accuracy is a function of the land cover, accuracy over bare soils was also computed and LE68 and LE90 of 1.5 m and 3.5 m respectively, were obtained. DTM accuracy is also linearly correlated with the terrain slopes.

Since the DTM is in fact a DSM (including surface heights), two methods for extracting the buildings in 3D were presented. Preliminary results show a good potential using an expert system and some general characteristics about the buildings (maximum and minimum heights and surfaces).

ACKNOWLEDGMENTS

The authors would like to thank ImageSat International for EROS-A1 images, SpaceImaging for IKONOS image over Toronto, Canada and DigitalGlobe for QuickBird-2 images. They also thank Dr. Philip Cheng for porting CCRS 3D parametric model for high-resolution images in OrthoEngine[SE] of PCI Geomatics inc.

REFERENCES

Fraser, C.S. Baltsavias E. & Gruen A. Processing of Ikonos imagery for submetre 3D positioning and building extraction. *ISPRS Journal of photogrammetry & Remote Sensing*, Vol. 56 (No. 3): 177-194.

Hofman P. 2001. Detecting buildings and roads from IKONOS data using additional information. *GIS Geo-Informations-Systeme* Vol. 6: 28-33

Toutin, Th. 1995. Multi-source Data Integration with an Integrated and Unified Geometric Modelling. *EARSeL Journal "Advances in Remote Sensing*, Vol. 4 (No. 2): 118-129.

Toutin, Th. 2001. *Geometric processing of IKONOS Geo images with DEM. Proceedings of ISPRS Joint Workshop "High Resolution Mapping form Space", Hannover, Germany, September 19-21, CD-ROM:* 264-271.

Toutin, Th. & Cheng P. 2000. Demystification of IKONOS. *Earth Observation Magazine* July, Vol. 9, (No. 7): 17-21.

Toutin, Th. Chénier R. & Carbonneau Y. 2001. *3D Geometric modelling of IKONOS Geo Images. Proceedings of ISPRS Joint Workshop "High Resolution Mapping form Space", Hannover, Germany, September 19-21, CD-ROM*: 272-280.

Weidner U. & Förstner W. 1995. Towards automatic extraction from high-resolution digital elevation models, *ISPRS Journal of Photogrammetry & Remote Sensing* Vol. 50, (No. 4):38-49.